TMC-95A Analogues with Endocyclic Biphenyl Ether Group as Proteasome Inhibitors

by **Markus Kaiser**[a]), **Alexander G. Milbradt**[a]), **Carlo Siciliano**[a]), **Irmgard Assfalg-Machleidt**[b]), **Werner Machleidt**[b]), **Michael Groll**[a])[1]), **Christian Renner**[a]), and **Luis Moroder***[a])

[a]) Max-Planck-Institut für Biochemie, AG Bioorganische Chemie, Am Klopferspilz 18A, D-82152 Martinsried (phone: 49-89-8578-3905, fax: 49-89-8578-2847, e-mail: moroder@biochem.mpg.de)

[b]) Adolf-Butenandt-Institut der Ludwig-Maximilians-Universität, D-80336 München

TMC-95A, a cyclic tripeptide metabolite of *Apiospora montagnei*, is a potent competitive inhibitor of proteasome. Based on the X-ray structure of its complex with yeast proteasome, the synthetically challenging structure of this natural product was simplified in a first generation of analogues by replacing the highly oxidized side-chain biaryl system with a phenyl-oxindole group. In the present study, the TMC-95 biaryl group was substituted with a biphenyl ether with retainment of significant proteasome inhibition. Because of the facile synthetic access of tripeptides containing in i, $i+2$ positions residues of the isodityrosine type, this new generation of TMC-95 analogues may represent promising lead structures for further optimization of affinity and selectivity of proteasome inhibitors.

1. Introduction. – In eukaryotes, the ATP-dependent ubiquitin-proteasome pathway is the major intracellular proteolytic machinery and, therefore, key to activation or repression of many cellular processes such as cell-cycle progression and apoptosis. It is responsible for degradation of misfolded, damaged, and aged proteins, for elimination of regulatory proteins, and plays a central role in the cellular immune response by antigenic peptide processing [1–3]. Because of this crucial control of vital processes, a selective inhibition of the proteasome is of promising therapeutic potential for treatment of cancer, inflammatory disorders, and immune diseases [1][2][4][5].

The proteasome consists of a 20S proteolytic core particle and a 19S regulatory subunit at either one or both ends [6–8]. The regulatory particle 19S is responsible for binding the poly-ubiquitinated proteins, and for their unfolding and translocation to the proteolytic 20S core particle. This core particle is a multicatalytic enzyme characterized by a conserved structure in virtually all organisms from archaebacteria [9][10] to yeast [11] and humans [12]: a hollow barrel-shaped architecture formed by four stacked $\alpha_{1-7}\beta_{1-7}\beta_{1-7}\alpha_{1-7}$ multiprotein rings. In the eukaryotic 20S proteasome, only $\beta1$, $\beta2$, and $\beta5$ of the seven β-subunits, present in duplicate in the two central rings, are autolytically processed during maturation with release of the N-terminal threonine as the functional nucleophile of the enzyme active sites, which degrade in processive manner the proteins into small-size peptides [13]. Each proteolytically active subunit shows a certain degree of substrate specificity with $\beta1$ for post-glutamyl peptide hydrolysis (PGPH), $\beta2$ for

[1]) Present address: Institut für Physiologische Chemie, Ludwig-Maximilians-Universität München, Butenandtstrasse 5, D-81377 München.

trypsin-like (TL), and $\beta5$ for chymotrypsin-like (CL) activity as well assessed by mutational and crystallographic studies [14–16].

In addition to synthetic peptide aldehydes [17], boronates [18], and vinyl sulfones [19][20], various metabolites from microorganisms were discovered as efficient inhibitors of the proteasome such as lactacystin [21], the epoxy ketones epoxomicin [22] and eponemycin [23], and the TMC-95A and its diastereoisomers TMC-95B/C/D [24][25]. All of these inhibitors lead to covalent modification of the N-terminal threonine of the β-subunits [2][9][11][26][27], except the TMC-95 compounds. The reversible inhibition mechanism of TMC-95 makes these natural products of particular interest as lead structures for drug development.

The four TMC-95 diastereoisomers are cyclic tripeptide derivatives containing a biaryl system constrained into a 17-membered heterocycle (*Fig. 1*; **1**), and its binding mode has been characterized by X-ray crystallography [27]. In the TMC-95A/yeast proteasome complex the non-covalent interactions are mainly mediated by H-bonds between the extended peptide backbone and the protein counterpart in a manner similar to an antiparallel β-sheet. Thereby, the C-terminal (*Z*)-propenyl moiety acts as P1 and the asparagine as P3 residue, whereas the N-terminal keto-amide group is largely exposed to the surface without apparent interactions with the protein. From these structural data, a significantly simplified analogue (*Fig. 1*; **2**) of TMC-95A was derived, which was found to retain inhibitory activities [28]. The N-terminal 3-methyl-2-oxopentanoyl and the synthetically challenging C-terminal (*Z*)-(prop-1-enyl)amino

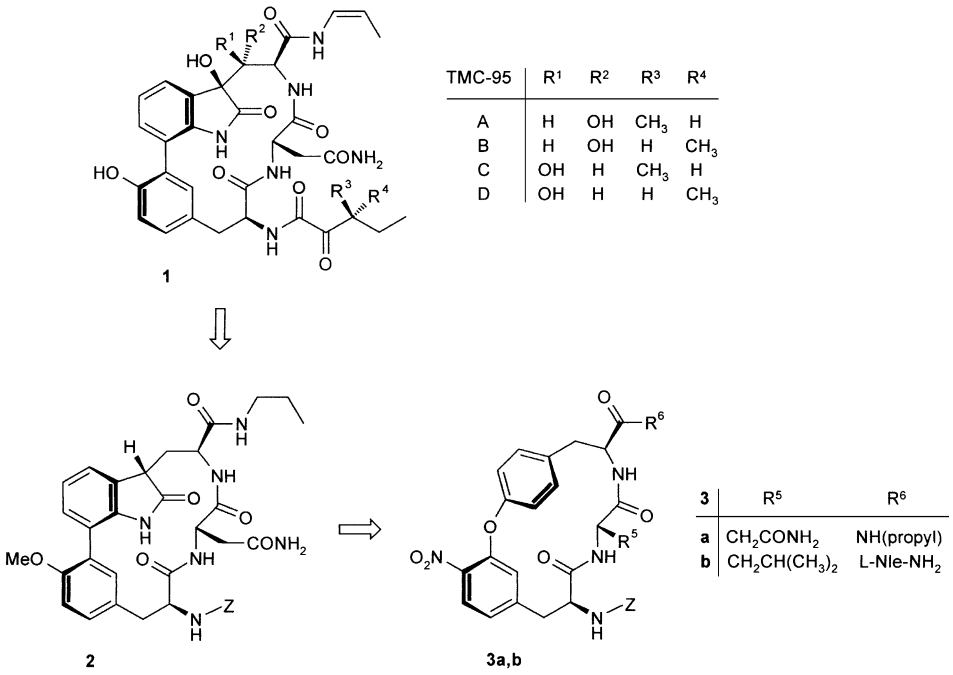

Fig. 1. *Structures of the natural TMC-95 products* **1** *and of related analogues with endocyclic phenol-oxindole* [28], *and biaryl ether groups,* **2** *and* **3a**,**b**, *respectively*

groups were replaced by (benzyloxy)carbonyl (*Z*) and propylamino groups, respectively, and the highly oxidized form of the tryptophan could be reduced to β-(2-oxoindol-3-yl)alanine, which, however, proved to be essential for efficient ring closures of the biaryl-containing linear precursor *via* the macrolactamization approach [28] as well as of suitable peptide derivatives *via* intramolecular side-chain *Suzuki* cross-coupling [29].

According to the X-ray analysis of the proteasome/TMC-95A complex, the main role of the phenol-oxindole biaryl system appears to be induction and stabilization of an extended β-type peptide-backbone conformation [27]. Biaryl ethers of the isodityrosine type are known to induce the identical conformational restriction when used as structural clamps in positions *i*, $i+2$ of cyclic peptides [30–32]. Therefore, replacement of the phenol-oxindole group in TMC-95A with an endocyclic biaryl ether could further facilitate the synthetic access of TMC-95A analogues as potential proteasome inhibitors. As confirmation of principle, in the present study such a replacement with biaryl ether was attempted, and the resulting TMC-95A analogues **3a** and **3b** (*Fig. 1*) were found to exhibit promising inhibitory properties.

2. Results. – 1. *Design of the Biaryl Ether Analogues of TMC-95A.* To retain the 17-membered cyclic structure of TMC-95A, the biphenyl ether junction can be established by *para-meta* or *meta-para* substitutions in the biphenyl ether when viewed from the N- to the C-terminus. Therefore, both endocyclic junctions were analyzed by modelling experiments and compared to TMC-95A. A superimposition of the resulting structures on that of the proteasome-bound TMC-95A inhibitor (*Fig. 2*) clearly revealed highly constrained geometries for both structural models. Although the backbone conformations of all three molecules are quite similar, on closer inspection an almost perfect match of the backbones is observed for TMC-95A and the *meta-para* linked biphenyl

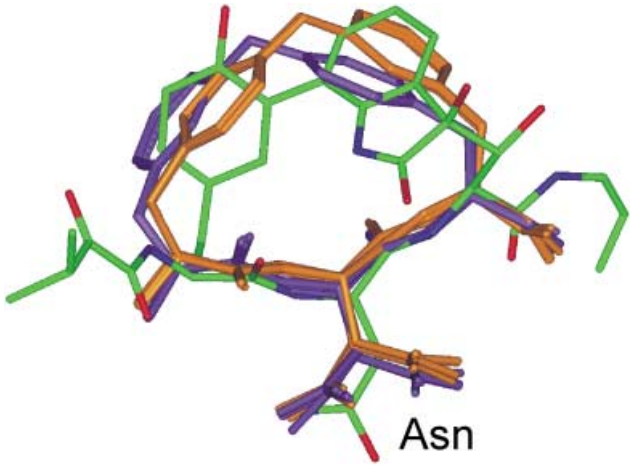

Fig. 2. *Superimposition of the ten lowest-energy structures resulting from modelling calculations for the* para-meta (orange) *and* meta-para (violet) *linkage on the natural TMC-95A inhibitor*. In the structural models, only the central three amino acid residues are shown (the N-terminal Z group and C-terminal Pr chain are omitted).

ether, whereas small but recognizable differences exist in a comparison of TMC-95A and the *para-meta* version. The positions and orientations of the aromatic side-chain rings differ considerably. However, this is expected to be less important as the aromatic side chains of TMC-95A are mostly solvent-exposed in the crystal structure.

Correspondingly, compounds **3a** and **3b** (*Fig. 1*) were selected as target molecules. In analogy to compound **2** as representative of the first generation of TMC-95A analogues, the N-terminus of the tripeptide was blocked as (benzyloxy)carbonyl (*Z*) derivative and the C-terminal (*Z*)-(prop-1-enyl)amino group was replaced with propylamino group as P1 residue, while the central asparagine residue was retained as P3. In compound **3b**, the asparagine was replaced with leucine and the C-terminal propylamino group with norleucine amide as P1 residue in analogy to the calpain inhibitor I, *i.e.*, the peptide aldehyde Ac-Leu-Leu-Nle-H [17]; even for peptide vinyl sulfones, such P1 and P3 residues were found to be optimal for inhibition of the CL activity of the proteasome [20].

2. *Synthesis of the Biaryl Ether-Cross-Bridged Cyclic Peptides* **3a** *and* **3b**. Among the various methods elaborated for the synthesis of biaryl ethers [33–41], the procedure of *Beugelmans et al.* [40] is based on the nucleophilic attack of the phenol on a fluorobenzene derivative activated by an *ortho*-NO_2 group. This procedure has been successfully applied also in syntheses on solid supports [42]. Since the phenolic group is largely solvent-exposed in the TMC-95A/proteasome complex, reaction of a tyrosine residue as P2 with a (3-F,4-NO_2)-phenylalanine as P4 was selected for the ring closure.

2.1. *Synthesis of Compound* **3a** *in Solution*. The key intermediate methyl (*S*)-3-fluoro-4-nitrophenylalaninate (**4**) was obtained by the method of *Beugelmans et al.* [40]. As shown in *Scheme 1*[2]), the methyl ester **4** was protected as *N*-Z derivative and saponified to yield **5**. On the other hand, Boc-Tyr-OH was transformed by standard procedures into the *N*-propyl-amide derivative **6**, which was N^{α}-deprotected with TFA, converted to the corresponding triisopropylsilyl (TIPS) ether, and then coupled with Boc-Asn-OH by the EDCI/HOBt method to produce the intermediate **7**. N^{α}-Deprotection of **7** and coupling with **5** led to the linear intermediate **8**, which, in turn, was macrocyclized *via* intramolecular nucleophilic aromatic substitution by exposure to TBAF. Reversed-phase HPLC provided the desired cyclic compound **3a** in 13% yield from the cyclization step.

2.2. *Synthesis of Compound* **3b** *on Resin*. The synthesis was performed by the Fmoc strategy on *Rink*-amide resin by stepwise coupling of Fmoc-amino acids with TBTU/HOBt and PyBOP/HOBt, respectively, and intermediate Fmoc cleavage with 20% piperidine in NMP, as shown in *Scheme 2*[2]). Protection of the Tyr side chain as TIPS ether was performed with TIPSOTf and 1*H*-imidazole as base. The concomitant silylation of the amino group led to its activation for the subsequent acylation step with **5**. Simultaneous deprotection of the Tyr residue and ring closure with TBAF, followed by acidolytic cleavage from the resin, afforded the cyclic compound **3b** in 9% overall yield after reversed-phase HPLC purification.

3. *Inhibition of Yeast Proteasome by the TMC-95A Analogues.* Since TMC-95A was not available for comparative analysis of the inhibitory potencies of the analogues, the calpain inhibitor I was used as standard, and a newly optimized enzyme assay was

---

[2]) For abbreviations, *cf.* the *Exper. Part.*

Scheme 1. *Synthesis of the Cyclic Peptide* **3a**

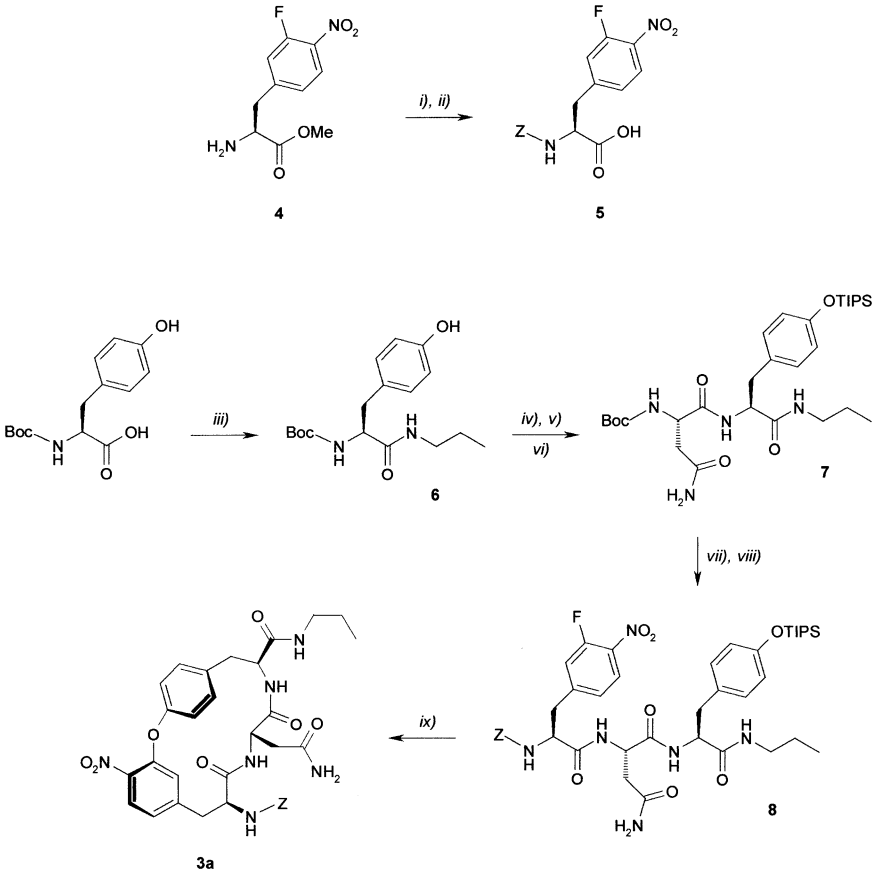

i) Z-OSu, $NaHCO_3$, 1,4-dioxane/H_2O 1:1, r.t., overnight; 98%. *ii*) LiOH, MeCN/H_2O 3:1, r.t., overnight; 89%. *iii*) $PrNH_2$, HOBt, EDCI, DIEA, DMF, r.t., overnight; 92%. *iv*) TFA/CH_2Cl_2 1:1, r.t., 2 h; 98%. *v*) TIPSOTf, 1*H*-imidazole, DIEA, CH_2Cl_2, r.t., 3 h; 91%. *vi*) Boc-Asn-OH, HOBt, EDCI, DIEA, DMF, r.t., overnight, 89%. *vii*) TFA/CH_2Cl_2 1:1, r.t., 2 h, 96%. *viii*) **5**, HOBt, EDCI, DIEA, DMF, r.t., overnight, 90%. *ix*) TBAF, THF, r.t., 14 h; 13 %.

applied to determine the K_i values for the CL, TL, and PGPH activities of yeast proteasome (*Table*). A comparison of the inhibitory potencies of compounds **2** and **3a** with the K_i values of the Ac-Leu-Leu-Nle-H as reference clearly revealed that binding affinities for the β2 and β5 active sites of yeast proteasome, *i.e.*, inhibition of the TL and CL activities, were largely retained by the TMC-95 analogues, despite the different biaryl system used as endocyclic cross-bridge, thus confirming the working hypothesis. A replacement of the propyl residue and asparagine of **3a** with norleucine as P1 and leucine as P3 residue in the cyclic peptide **3b** generated an analogue with surprisingly high selectivity for the β5 subunit of yeast proteasome, although its affinity for this active site, and thus inhibition of the CL activity was twelvefold reduced compared to **3a**.

Scheme 2. *Synthesis of the Cyclic Peptide* **3b** *on Resin*

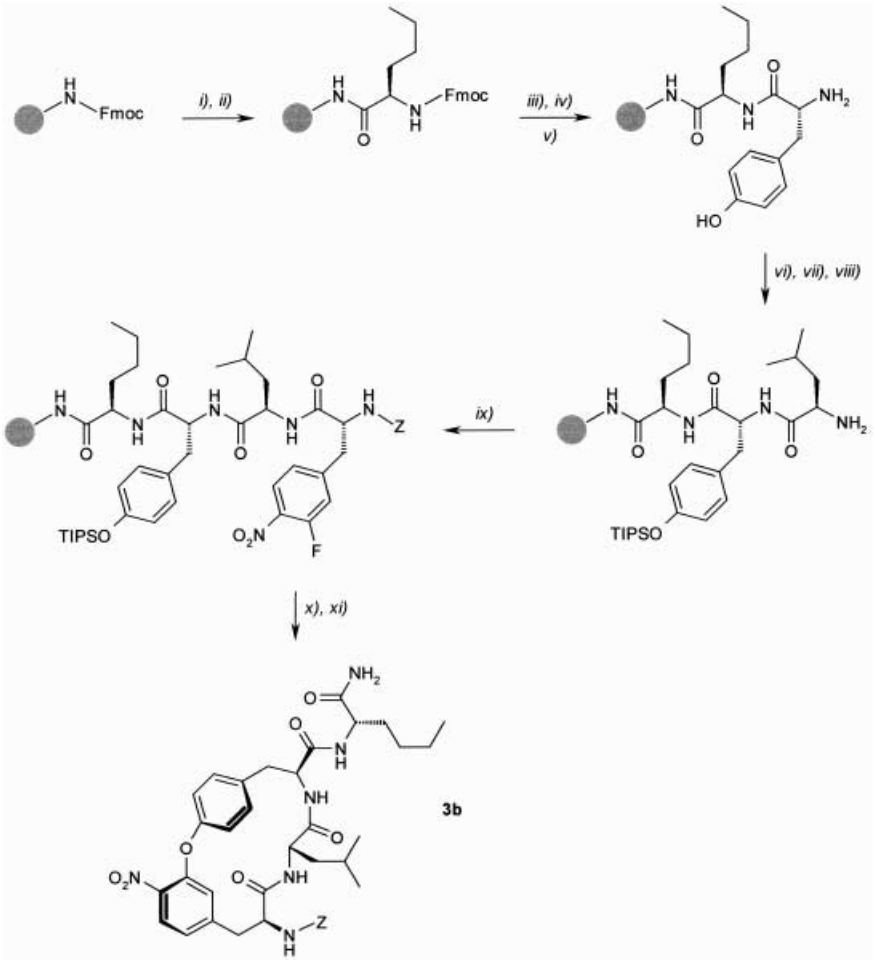

i) NMP/piperidine 4 : 1, 30 min. *ii*) Fmoc-Nle-OH, HOBt, TBTU, DIEA, NMP, 4 h. *iii*) NMP/piperidine 4 : 1, 30 min. *iv*) Fmoc-Tyr-OH, HOBt, TBTU, DIEA, NMP, 4 h. *v*) NMP/piperidine 4 : 1, 30 min. *vi*) TIPSOTf, 1*H*-imidazole, CH_2Cl_2, 3 h. *vii*) Fmoc-Leu-OH, HOBt, TBTU, DIEA, NMP, 4 h. *viii*) NMP/piperidine 4 : 1, 30 min. *ix*) **5**, HOBt, PyBOP, DIEA, NMP, 6 h. *x*) TBAF, THF, 2 d. *xi*) 95% aq. TFA, 1 h.

Table. *Inhibition of Yeast Proteasome* (K_i [μM]) *by TMC-95 Analogues*

Inhibitor	CL Activity	TL Activity	PGPH Activity
Ac-Leu-Leu-Nle-H	1.4	364	$\geq$2000
2	2.4	55	$\geq$2000
3a	5.5	74	$\geq$2000
3b	65	$\geq$2000	$\geq$2000

4. *NMR Structural Analysis of the Cyclic Peptides* **3a** *and* **3b**. To further investigate the structural effect of the biaryl ether system on the peptide backbone, a conformational analysis was performed on the compounds **3a** and **3b**. Well-resolved spectra recorded in DMSO at 22° allowed the extraction of sufficient experimental NOE distance constraints for calculation of highly convergent structures (*Fig. 3*). The ten lowest energy structures have a backbone rmsd for the central tripeptide of 0.45 Å for **3a** and 0.09 Å for **3b**. Also, the aromatic side chains are very well-defined with heavy atom rmsd for both aromatic amino acids of 0.55 Å for **3a** and 0.10 Å for **3b**. By comparing the structure derived for **3a** with that of the proteasome-bound TMC-95A and the simplified analogue **2** (*Fig. 4*), it is evident that the C-terminal propyl chain as P1 residue differs in its orientation both from the (*Z*)-prop-1-enyl group of the natural product and the alkyl chain in **2**. However, the extended β-type conformations of the peptide backbones show a high degree of convergence in the three cyclic peptides, a fact that may primarily be responsible for their ability to inhibit the proteasome CL and TL activity with similar potencies, although the biaryl ether clamp is apparently less efficient for juxtaposition of the backbone for optimal alignment with the active-site clefts of the β-subunits. In the case of compound **3a**, less-optimal recognition can be explained by the backbone dihedral angle ϕ of asparagine differing by *ca.* 50° from the natural inhibitor and the two synthetic analogues **2** and **3b**, which share similar values. For **3b**, on the other hand, the rather flexible norleucine side chain as P1 residue results in an entropic penalty and might even be unfavorable in steric terms. Additionally, compound **3b** is very poorly recognized by the trypsin-like active site of the β2 subunit because the leucine residue replacing asparagine, although similarly oriented (*Fig. 3*), is unpolar.

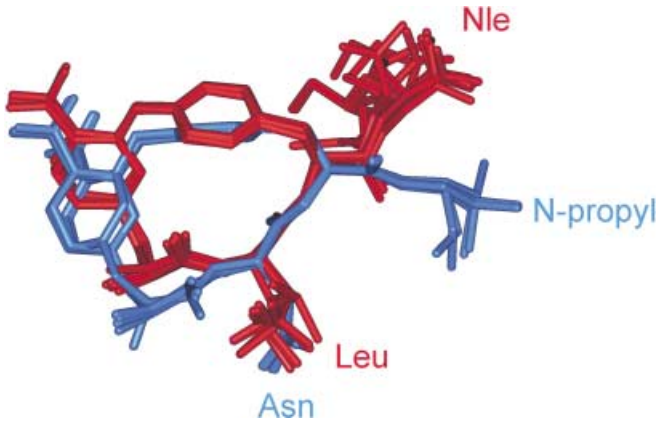

Fig. 3. *Comparison of NMR structures of the biphenyl ether compounds* **3a** (blue) *and* **3b** (red). The ten lowest-energy structures of each are superimposed on the heavy atoms of the aromatic amino acids. In both cases, the N-terminal Z group is omitted for clarity.

3. Discussion. – The strong pore restriction of the 20S proteasome allows only for translocation of linear unfolded polypeptide chains into the proteolytic chamber, whereas disulfide-bridged cyclic peptides are not degraded by the proteasome [43].

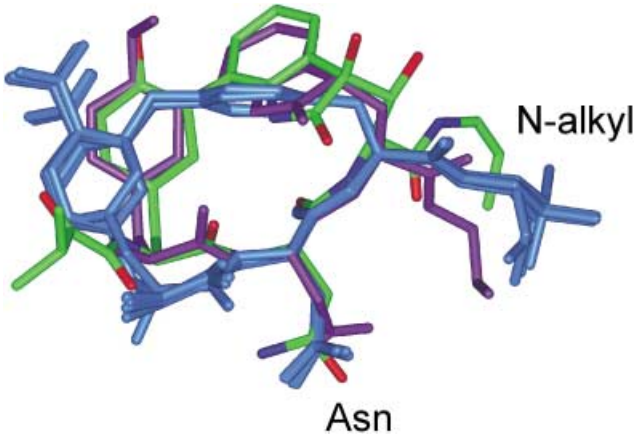

Fig. 4. *Superimposition of NMR structures of the TMC analogue* **2** (violet) *and the biphenyl ether compound* **3a** (blue) *on the structure of the natural TMC-95A inhibitor* (atom colors) *in the crystallized complex* [27]. For **3a**, the ten lowest-energy structures resulting from NMR structure calculations are shown, whereas, for **2**, only one representative of the highly convergent NMR structure ensemble is encluded. For **2** and **3a**, the N-terminal Z group is omitted.

Despite a cyclic structure, peptides of the TMC-95 type are apparently able to enter into the large cavity of the 20S particle, as documented by their efficient inhibition of the enzyme. This has to be ascribed to the relatively small 17-membered ring size, which preorganizes the tripeptide backbone by conformational restriction into a β-type extended structure for its binding to the active-site clefts with a minimum of entropic penalty. In crystals of the Ac-Leu-Leu-Nle-H/proteasome [11] and TMC-95A/proteasome complexes [27], all β1, β2, and β5 subunits are occupied by the inhibitors despite the low inhibition of the β1 subunit (PGPH activity) by the peptide aldehyde (see the *Table*) and by TMC-95A [28]. This has to be attributed to the high inhibitor concentration used in the crystallization experiments.

From the crystal structure of the TMC-95A/proteasome complex, mainly interactions between the peptide backbone and the active-site clefts were identified as possibly responsible for the binding affinity, whereas, for the N-terminal ketoamide group and the rest of the bulky biaryl group, significant interactions could not be observed. The surprisingly similar CL and TL inhibitory potencies of compounds **2** and **3a** with the oxindole-phenol and biphenyl ether system, respectively, would support a similar scaffold-like function of the two side-chain junctions and, in addition, minimize the contribution of the oxindole H-bond observed in the TMC-95A/proteasome complex. Based on these findings, it is reasonable to assume that the significantly reduced inhibition of the β2 subunit by compound **2** compared to TMC-95A [28] has to be correlated with replacement of the C-terminal (*Z*)-prop-1-enyl chain with the more-flexible propyl group. This conclusion is in full agreement with results obtained by similar replacements of the P1 residue in TMC analogues containing the intact core structure of the natural product [44]. Similarly, replacement of the propyl group by the larger and even more-flexible norleucine side chain leads to a further reduction in binding affinity for the β2 subunit, but concurrently also to some loss of affinity for the

β5 subunit and thus to a highly selective, although not very potent, inhibitor of the chymotryptic-like activity of the proteasome. However, the findings are encouraging, since solid-phase synthesis of such biaryl-ether-bridged tripeptides should allow for an iterative design of inhibitors with ameliorated binding affinities.

In such a design of new proteasome inhibitors, the main concern may be the loss of proteasome selectivity as shown by the TMC-95 natural products [24]. In fact, other natural products containing the biaryl-ether junction such as the tripeptide derivatives K13 [45][46] or OF 4949-I-IV [47][48] are known inhibitors of metalloproteases. These differ in their structure from the biaryl-ether compounds of this study merely by the presence of a C-terminal carboxy group as the potential ligand of the enzyme metal ion.

Experimental Part

General. All reagents and solvents were purchased from *Aldrich* and *Fluka* (*Sigma-Aldrich Chemie GmbH*, D-Deisenhofen), *Merck* (D-Darmstadt), and *Lancaster* (*Lancaster Synthesis GmbH*, D-Mühlheim a. M.), and were used without further purification. *TentaGel-S-RAM* (linker: 4-[(*R*,*S*)-α-amino-2′,4′-dimethoxybenzyl]-phenoxyacetic acid) was from *Rapp Polymere GmbH* (D-Tübingen). TLC was carried out on silica-gel *60* F_{254} precoated glass plates (0.25-mm layer; *Merck*, D-Darmstadt). Anal. HPLC was performed with *Waters* equipments on *I*) *Symmetry* C_{18} *5 µm Chromolith* column (150 × 3.9 mm) from *Waters* by a linear gradient from 5% MeCN in 2% aq. H_3PO_4 to 90% MeCN in 2% aq. H_3PO_4 in 15 min (flow rate: 1.5 ml/min), and on *II*) *C18 5 µm* column (100 × 4.6 mm) from *Merck* (D-Darmstadt) by linear gradient elution from 5% MeCN in 2% aq. H_3PO_4 to 90% MeCN in 2% aq. H_3PO_4 in 7 min (flow rate: 3 ml/min); t_R are reported in min. Prep. RP-HPLC was performed on *Abimed-Gilson* chromatograph with a *Nucleosil* C_8 *SP250/10* column (*Macherey & Nagel*, D-Düren) and gradients from 0.1% aq. TFA to MeCN containing 0.1% TFA (flow rate: 3 ml/min). Melting points were determined on a *Büchi 510* apparatus (*Büchi Laboratoriums-Technik AG*, CH-Flawil), and are uncorrected. Optical rotations were determined on a *Perkin-Elmer 241 mc* polarimeter. Routine ^{1}H- and ^{13}C-NMR spectra were recorded on a *Bruker AMX-400* spectrometer (*Bruker*, D-Karlsruhe). Chemical shifts δ are reported in ppm relative to Me_4Si as internal standard; *J* values in Hz. NMR experiments for conformational analysis were carried out at 22° on a *Bruker DRX-500* spectrometer (*Bruker*, D-Karlsruhe). LC-ESI mass spectra were recorded on a *PE Sciex API165* instrument, equipped with a *Microgradient System 140C* (*Applied Biosystems*), a *PE 785A* UV/VIS Detector, a *PE Series 200* autosampler and a *PE Nelson 200* interface with a *Nucleosil* C_8 100/5 column (125 × 2 mm) and a linear gradient from 5% MeCN in 0.05% aq. TFA to 90% MeCN in 0.05% aq. TFA in 15 min (flow rate: 250 µl/min).

Abbreviations. Standard abbreviations are used as recommended by the IUPAC-IUB commission on biochemical nomenclature and the ACS Style Guide. All amino acids are of L-configuration. Additional abbreviations: CVFF, Consistent Valence Force Field; DQF-COSY, Double Quantum Filtered COrrelation SpectroscopY; TOCSY, TOtal Correlation SpectroscopY; ROESY, Rotating-frame Overhauser Enhancement SpectroscopY; PyBOP, (benzotriazol-1-yloxy)tris(pyrrolidino)phosphonium hexafluorophosphate; EDCI, *N*′-ethyl-*N*″-[3-(dimethylamino)propyl]carbodiimide hydrochloride; HBTU, 2-(1 H-benzotriazol-1-yl)-1,1,3,3-tetramethyluronium hexafluorophosphate; Z-OSu, *N*-[(benzyloxy)carbonyloxy]succinimide, TIPSOTf, triisopropylsilyl trifluoromethanesulfonate; HOBt, 1-hydroxybenzotriazole; TBAF, tetrabutylammonium fluoride; DIEA, (diisopropyl)(ethyl)amine; TFA, trifluoroacetic acid; NMP, *N*-methylpyrrolidin-2-one.

*(*S*)-*N*-[(Benzyloxy)carbonyl]-3-fluoro-4-nitrophenylalanine* (**5**). To a soln. of methyl 3-fluoro-4-nitrophenylalaninate hydrochloride [40] (120 mg, 0.495 mmol) in 1,4-dioxane/H_2O 1:1 (15 ml) Z-OSu (136 mg, 0.545 mmol) and $NaHCO_3$ (46 mg, 0.545 mmol) were added. After stirring at r.t. for 12 h, *N*-(2-aminoethyl)piperazine (100 µl) was added, and the mixture was stirred for an additional 30 min. The bulk of the solvent was evaporated, and the residue was poured into AcOEt (10 ml), and washed with 5% $NaHCO_3$ soln. (3 × 10 ml), 5% $KHSO_4$ soln. (3 × 10 ml), and brine (10 ml). The org. layer was dried (Na_2SO_4) and evaporated to dryness to afford the N^{α}-protected methyl ester (190 mg, 98%). TLC ($CHCl_3$/MeOH 9:1): R_f 0.32. HPLC (*I*): t_R 10.1. ES-MS: 377.3 ($[M+H]^+$; $C_{18}H_{17}FN_2O_6^+$; calc. 376.34).

The methyl ester (190 mg, 0.505 mmol) was saponified in MeCN/H_2O 3:1 (20 ml) with LiOH (32 mg, 0.76 mmol). After 12 h, the soln. was acidified with 5% $KHSO_4$ soln. (3 ml), concentrated, and distributed between 5% $KHSO_4$ soln. (10 ml) and AcOEt (10 ml). The aq. layer was extracted with AcOEt (2 × 10 ml), and

the combined org. extracts were washed with brine (10 ml), dried (Na_2SO_4), and evaporated to dryness to yield **5** (163 mg, 89%). Pale yellow solid. M.p. 122–125°. $[\alpha]_D^{20} = +28.82$ ($c = 1$, MeOH). TLC ($CHCl_3$/MeOH 9:1): R_f 0.58. HPLC (*I*): t_R 8.85. ^{1}H-NMR (400 MHz, (D_6)DMSO, 27°): 2.98 (*dd*, $J = 11.1, 14.7$, 1 H, $\beta CH_2^{Tyr(3F,4NO2)}$); 3.22 (*dd*, $J = 4.28, 14.7$, 1 H, $\beta CH_2^{Tyr(3F,4NO2)}$); 4.31 (*ddd*, $J = 4.28, 8.4, 11.1$, 1 H, αCH); 4.97 (*s*, 2 H, PhCH_2); 7.27–7.39 (*m*, 6 H, Ph, ArH); 7.49 (*d*, $J = 8.4$, 1 H, NH); 7.72 (*d*, $J = 8.7$, 1 H, ArH); 8.07 (*m*, 1 H, ArH); 11.02 (*s*, 1 H, CO_2H). ^{13}C-NMR (100 MHz, (D_6)DMSO, 27°): 36.25; 54.67; 65.53; 118.98; 119.19; 126.29; 127.67; 127.94; 128.42; 137.12; 148.39; 148.48; 155.76; 172.81. ES-MS: 363.3 ($[M+H]^+$, $C_{17}H_{15}FN_2O_6^+$; calc. 362.32).

Boc-Tyr-NHPr (**6**). To a precooled soln. of Boc-Tyr-OH (2.0 g, 7.1 mmol) in DMF (60 ml) were added HOBt (1.31 g, 8.54 mmol), EDCI (1.44 g, 7.4 mmol), $PrNH_2$ (0.88 ml, 10.67 mmol), and DIEA (1.22 ml, 7.1 mmol). After overnight stirring at r.t., the mixture was evaporated, the residue was dissolved in AcOEt (20 ml) and washed with 5% $KHSO_4$ soln. ($3 \times$ ml 20), 5% $NaHCO_3$ soln. (3×20 ml), and brine (20 ml). The soln. was dried (Na_2SO_4) and evaporated to dryness to afford **6** (2.1 g, 92 %). White powder. M.p. 137–140°. $[\alpha]_D^{20} = +32.54$ ($c = 1$, MeOH). TLC ($CHCl_3$/MeOH 8:2): R_f 0.49. HPLC (*II*): t_R 2.6. ^{1}H-NMR (400 MHz, (D_6)DMSO, 27°): 0.80 (*t*, 3 H, CH_2CH_2*Me*); 1.36 (*s*, 9 H, Me_3C); 1.39 (*m*, 2 H, CH_2CH_2Me); 2.62 (*dd*, $J = 4.8, 13.1$, 1 H, βCH_2^{Tyr}); 2.79 (*dd*, $J = 11.9, 13.1$, 1 H, βCH_2^{Tyr}); 2.98 (*m*, 2 H, CH_2CH_2Me); 4.04 (*m*, 1 H, αCH); 6.63 (*d*, $J = 8.12$, 2 H, Ar*H*); 6.72 (*d*, $J = 7.87$, 1 H, N*H*); 7.01 (*d*, $J = 8.12$, 2 H, Ar*H*); 7.55 (*m*, 1 H, PrN*H*); 9.14 (*s*, 1 H, OH). ^{13}C-NMR (100 MHz, (D_6)DMSO, 27°): 21.77; 28.08; 28.61; 56.22; 78.12; 114.97; 115.82; 128.33; 130.08; 130.32; 155.32; 155.89; 171.71. ES-MS: 322.4 ($[M+H]^+$, $C_{17}H_{26}N_2O_4^+$; calc. 322.41).

Boc-Asn-Tyr(OTIPS)-NHPr (**7**). Compound **6** (1.1 g, 3.3 mmol) was dissolved in TFA/CH_2Cl_2 1:1 (15 ml) and kept for 2 h at r.t. The soln. was taken to dryness, and the residue was evaporated twice from toluene (10 ml) and then dissolved in CH_2Cl_2 (40 ml). To the resulting soln. were added DIEA (0.56 ml, 3.28 mmol), 1*H*-imidazole (0.67 g, 9.85 mmol), and TIPSOTf (1.76 ml, 6.56 mmol). After 3 h at r.t., the mixture was evaporated, the residue was dissolved in AcOEt (20 ml) and washed with 5% $KHSO_4$ soln. (3×20 ml), 5% $NaHCO_3$ soln. (3×20 ml), and brine (20 ml). The org. layer was dried (Na_2SO_4), evaporated to dryness, and dissolved in DMF (20 ml). To this soln., Boc-Asn-OH (1.14 g; 4.92 mmol) was added, followed by DIEA (0.85 ml; 4.92 mmol), HOBt (0.75 g; 4.92 mmol), and EDCI (0.94 g; 4.92 mmol). After stirring overnight at r.t., the mixture was concentrated to a small volume, diluted with AcOEt (30 ml), washed with 5% $NaHCO_3$ soln. (3×20 ml), 5% $KHSO_4$ soln. (3×20 ml), and brine (20 ml), and dried (Na_2SO_4) and evaporated to dryness to yield pure **7** (1.7 g, 89%). White glassy solid. M.p. 136–139°. $[\alpha]_D^{20} = +75.33$ ($c = 1$, MeOH). TLC ($CHCl_3$/MeOH 8:2): R_f 0.51. HPLC (*II*): t_R 5.31. ^{1}H-NMR (400 MHz, (D_6)DMSO, 27°): 0.79 (*t*, $J = 7.73$, 3 H, CH_2CH_2*Me*); 1.05 (*d*, $J = 7.81$, 18 H, *Me*$_2$CH); 1.21 (*sept.*, $J = 7.81$, 3 H, Me_2C*H*); 1.37 (*sext.*, $J = 7.73$, 2 H, CH_2CH_2Me); 1.48 (*s*, 9 H, Me_3C); 2.37 (*dd*, $J = 10.6, 18.9$, 1 H, βCH_2^{Tyr}); 2.44 (*dd*, $J = 5.2, 12.9$, 1 H, βCH_2^{Tyr}); 2.72 (*dd*, $J = 10.9, 13.1$, 1 H, βCH_2^{Asn}); 2.92 (*dd*, $J = 5.8, 13.1$, 1 H, βCH_2^{Asn}); 2.99 (*t*, $J = 7.73$, 2 H, CH_2CH_2Me); 4.22 (*m*, 1 H, $\alpha CH^{Tyr(OTIPS)}$); 4.33 (*m*, 1 H, αCH^{Asn}); 5.38 (br. *s*, 2 H, $CONH_2$); 6.72 (*d*, $J = 8.22$, 2 H, ArH); 6.83 (*m*, 1 H, PrN*H*); 6.96 (*d*, $J = 8.1$, NH); 7.06 (*d*, $J = 8.22$, 2 H, ArH); 7.33 (*d*, $J = 7.9$, 1 H, NH). ^{13}C-NMR (100 MHz, (D_6)DMSO, 27°): 11.46; 12.22; 17.95; 22.32; 28.29; 36.92; 37.38; 40.56; 51.59; 54.32; 78.47; 119.27; 130.56; 155.23; 170.54; 171.22; 171.93. ES-MS: 593.8 ($[M+H]^+$, $C_{30}H_{52}N_4O_6Si^+$; calc. 592.86).

Z-Phe(3-F,4-NO$_2$)-Asn-Tyr(OTIPS)-NHPr (**8**). Compound **7** (200 mg, 0.338 mmol) was deprotected in CH_2Cl_2/TFA 1:1 (15 ml). After stirring 2 h at r.t., the soln. was taken to dryness, and the residue was evaporated from toluene (2×10 ml) to yield the intermediate trifluoroacetate salt as a white glassy solid in practically quant. yield. HPLC (*II*): t_R 3.73. ES-MS: 493.4 ($[M+H]^+$, $C_{25}H_{44}N_4O_4Si^+$; calc. 492.41).

To a soln. of **5** (100 mg, 0.275 mmol) in DMF (25 ml) were added DIEA (87 µl, 0.51 mmol), HOBt (50 mg, 0.33 mmol), and EDCI (55 mg, 0.29 mmol). After 10 min at r.t., a soln. of H-Asn-Tyr(OTIPS)-NHPr trifluoroacetate (134 mg, 0.220 mmol) in DMF (10 ml) was added, and the mixture was stirred overnight at r.t. The bulk of the solvent was evaporated, the residue was dissolved in AcOEt (20 ml) and washed with 5% $NaHCO_3$ soln. (3×20 ml), 5% $KHSO_4$ soln. (3×20 ml), and brine (20 ml). The org. extracts were dried (Na_2SO_4) and evaporated to dryness to yield **8** (165.5 mg, 90%). Pale yellow solid. M.p. 133–136°. $[\alpha]_D^{20} = +119.31$ ($c = 1$, MeOH). TLC ($CHCl_3$/MeOH 7:3): R_f 0.65. HPLC (*II*): t_R 5.61. ^{1}H-NMR (400 MHz, (D_6)DMSO, 27°): 0.78 (*t*, $J = 7.9$, 3 H, CH_2CH_2*Me*); 1.15 (*d*, $J = 7.7$, 18 H, *Me*$_2$CH); 1.26 (*sext.* $J = 7.9$, 2 H, CH_2CH_2Me); 1.42 (*sept.*, $J = 7.7$, 3 H, Me_2C*H*); 2.32–2.39 (*m*, 1 H, βCH_2^{Asn}); 2.57–2.64 (*m*, 1 H, βCH_2^{Asn}); 2.71–2.82 (*m*, 1 H, $CH_2^{Tyr(OTIPS)}$); 2.85–3.09 (*m*, 3 H, $CH_2^{Tyr(OTIPS)}$, $CH_2^{Tyr(3\text{-}F,4\text{-}NO2)}$); 3.31–3.44 (*m*, 2 H, CH_2CH_2Me); 4.25–4.36 (*m*, 2 H, $\alpha CH^{Tyr(OTIPS)}$, $\alpha CH^{Tyr(3\text{-}F,\,4\text{-}NO2)}$); 4.52–4.58 (*m*, 1 H, αCH^{Asn}); 4.65 (br. *s*, 2 H, NH_2); 4.77–5.01 (*m*, 2 H, PhCH_2); 6.61–6.73 (*m*, 3 H, ArH); 6.89 (*d*, $J = 6.8$, 1 H, NH); 7.18–7.42 (*m*, 5 H, ArH); 7.48–7.57 (*m*, 2 H, ArH); 7.84–7.97 (*m*, 2 H, ArH); 8.07 (*m*, 1 H, PrN*H*); 8.29 (*d*, $J = 8.8$, 1 H, NH); 8.43 (*d*, $J = 8.1$, 1 H, NH). ^{13}C-NMR (100 MHz, (D_6)DMSO, 27°): 11.47; 12.21; 17,88; 17.91; 22.31; 36.73; 37.35; 50.27; 53.94; 54.77; 65.61; 65.73; 119.28; 119.33; 126.03; 126.21; 127.91; 127.64; 128.38; 128.45; 130.15; 130.28; 130.42;

137.49; 137.58; 153.99, 155.91; 170.63; 170.51; 173.65; 173.72. ES-MS: 837.1 ($[M+H]^+$, $C_{42}H_{57}FN_6O_9Si^+$; calc. 837.13).

Benzyl 2-{[(9S,12S,15S)-12-(2-Amino-2-oxoethyl)-4-nitro-10,13-dioxo-15-[(propylamino)carbonyl]-2-oxa-11,14-diazatricyclo[15.2.2.1^{3,7}]docosa-1(19),3(22),4,5,17,20-hexaen-9-yl]amino}acetate (**3a**). To a stirred soln. of **8** (22 mg, 0.026 mmol) in THF (200 ml) was added dropwise a soln. of TBAF (33 mg, 0.105 mmol) in THF (30 ml). After 14 h at r.t., the solvent was removed, and the residue was dissolved in AcOEt (10 ml), washed with 5% $NaHCO_3$ soln. (3 × 10 ml), 5% $KHSO_4$ soln. (3 × 10 ml), and brine (10 ml). The org. layer was dried ($MgSO_4$) and evaporated to dryness. The crude product was precipitated from AcOEt with petroleum ether and purified by RP-HPLC to yield **3a** (2.3 mg, 13 %) after lyophilization from *t*-BuOH/H_2O 4 :1. HPLC (*II*): t_R 3.3. ^{1}H-NMR (500 MHz, (D_6)DMSO, 22°): 0.87 (*m*, 3 H, propylamide$^{H\gamma}$); 1.47 (*m*, 2 H, propylamide$^{H\beta}$); 2.43 (*m*, 2 H, Asn$^{H\beta}$); 2.54 (*m*, 1 H, Tyr$^{H\beta}$); 2.79 (*m*, 1 H, Phe$^{H\beta}$); 3.08 (*m*, 3 H, propylamide$^{H\alpha}$, Phe$^{H\beta}$); 3.24 (*m*, 1 H, Tyr$^{H\beta}$); 4.45 (*m*, 2 H, Phe$^{H\alpha}$, Tyr$^{H\alpha}$); 4.52 (*m*, 1 H, Asn$^{H\alpha}$); 5.01 (*d*, *J* = 12.7, 1 H, Z^{CH2}); 5.10 (*d*, *J* = 12.7, 1 H, Z^{CH2}); 6.01 (s, 1 H, Phe^{C2}); 6.25 (*d*, $J_{N\alpha}$ = 7.3, 1 H, Phe^{HN}); 6.65 (*d*, *J* = 7.3, 1 H, Phe^{C6}); 6.82 (*dd*, *J* = 8.5, *J* < 2, 1 H, Tyr^{C6}); 7.05 (*s*, 1 H, Z^{arom}); 7.10 (*dd*, *J* = 8.2, *J* < 2, 1 H, Tyr^{C5}); 7.25 – 7.45 (*m*, 6 H, Z^{arom}, Phe^{C2+C3}); 7.80 (*d*, *J* = 7.8, 1 H, Phe^{C5}); 8.11 (*t*, $J_{N\alpha}$ = 5.3, 1 H, propylamide^{NH}); 8.20 (*d*, $J_{N\alpha}$ = 10, 1 H, Tyr^{NH}); 8.26 (*d*, $J_{N\alpha}$ = 8.8, 1 H, Asn^{NH}). ES-MS: 661.7 ($[M+H]^+$, $C_{33}H_{36}N_6O_9^+$; 660.69).

Cyclic Peptide **3b**. Fmoc-*Tentagel-S-RAM* resin (518 mg, loading: 0.18 mmol/g, 0,093 mmol) was used and, after each reaction, washed with NMP (5 × 5 ml), i-PrOH (5 × 5 ml), DMF (3 × 5 ml), i-PrOH (3 × 5 ml), CH_2Cl_2 (3 × 5 ml), MeOH (3 × 5 ml), i-PrOH (3 × 5 ml), and Et_2O (3 × 5 ml), and then swollen in the solvent of the next reaction. The Fmoc-resin was deprotected with 20% piperidine in NMP (2 × 3 ml) for 5 min and 30 min, respectively. Coupling of Fmoc-Nle-OH (132 mg, 0.373 mmol), with TBTU (120 mg, 0.373 mmol), HOBt (57 mg, 0.373 mmol), and DIEA (128 µl, 0.746 mmol) was carried out in NMP (3 ml) for 4 h. The resin was washed, and the Fmoc group was removed by double treatment with 20% piperidine in NMP. After coupling of Fmoc-Tyr-OH (150 mg, 0.373 mmol) with TBTU (120 mg, 0.373 mmol), HOBt (57 mg, 0.373 mmol), and DIEA (128 µl, 0.746 mmol) in NMP (3 ml) for 4 h, Fmoc cleavage was performed as described above. The resin was reacted with 1*H*-imidazole (25 mg, 0.373 mmol), and TIPSOTf (100 µl, 0.373 mmol) in CH_2Cl_2 for 3 h. Fmoc-Leu-OH (132 mg, 0.373 mmol) was then coupled with TBTU (120 mg, 0.373 mmol), HOBt (57 mg, 0.373 mmol) and DIEA (128 µl, 0.746 mmol) in NMP (3 ml) for 4 h. From an aliquot of the resin (210 mg, 0.038 mmol), the Fmoc was removed as above, and **5** (32 mg, 0.088 mmol) was coupled with PyBOP (45 mg, 0.088 mmol), HOBt (6 mg, 0.088 mmol), and DIEA (30 µl, 0.174 mmol) in NMP (2 ml) for 6 h. After usual washings, the resin was reacted with TBAF (48 mg, 0.151 mmol) in THF (3 ml) for 2 d at r.t. Cleavage from the resin was performed with TFA/H_2O 95 :5 in 1 h, and the crude product was precipitated with petroleum ether and purified by prep. RP-HPLC to yield **3b** (2.5 mg, 9%) after lyophilization from *t*-BuOH/H_2O 4 :1. HPLC (*I*): t_R 10.01. ^{1}H-NMR (500 MHz, (D_6)DMSO, 22°): 0.83 (*m*, 6 H, Leu$^{\delta}$); 0.86 (*m*, 3 H, Nle$^{\varepsilon}$); 1.26 (*m*, 4 H, Nle$^{\gamma,\delta}$); 1.39 (*m*, 2 H, Leu$^{\beta}$); 1.51 (*m*, 1 H, Leu$^{\gamma}$); 1.56 – 1.66 (*m*, 2 H, Nle$^{\beta}$); 2.74 – 3.16 (*m*, 2 H, Phe$^{\beta}$); 2.57 – 3.21 (*m*, 2 H, Tyr$^{\beta}$); 4.23 (*m*, 1 H, Nle$^{\alpha}$); 4.38 (*m*, 1 H, Leu$^{\alpha}$); 4.41 (m, 1 H, Phe$^{\alpha}$); 4.57 (*m*, 1 H, Tyr$^{\alpha}$); 5.00 (*d*, *J* = 12.6, 1 H, Z^{CH2}); 5.08 (*d*, *J* = 12.6, 1 H, Z^{CH2}); 6.02 (*s*, 1 H, Phe^{C2}); 6.19 (*d*, $J_{N\alpha}$ = 7.3, 1 H, Phe^{NH}); 6.67 (*d*, *J* = 8.3, 1 H, Phe^{C6}); 6.80 (*dd*, *J* = 8.3, *J* < 2, 1 H, Tyr^{C5}); 7.09 (*dd*, 1 H, Tyr^{C3}); 7.30 (*dd*, *J* = 9.4, *J* < 2, 1 H, Tyr^{C6}); 7.08 (*s*, 2 H, C-term^{NH2}); 7.36 (*s*, 5 H, Z^{arom}); 7.45 (*dd*, 1 H, Tyr^{C2}); 7.79 (*d*, *J* = 8.3, 1 H, Phe^{C5}); 7.96 (*d*, $J_{N\alpha}$ = 8, 1 H, Nle^{NH}); 8.06 (*d*, $J_{N\alpha}$ = 9.2, 1 H, Leu^{NH}); 8.23 (*d*, $J_{N\alpha}$ = 10, 1 H, Tyr^{NH}). ES-MS: 731.8 ($[M+H]^+$, $C_{38}H_{46}N_6O_8^+$; calc. 730.83).

NMR Spectroscopy. Resonance assignments were performed according to the method of *Wüthrich* [49]. The 2D-TOCSY spectra were recorded with spin-lock periods of 75 ms with the MLEV-17 sequence for isotropic mixing [50]. Exper. interproton distance constraints (**3a**: 30, **3b**: 46) were extracted from a 2D-ROESY [51] experiment with a mixing time of 200 ms. ^3J(HN,Hα) couplings (**3a**: 4, **3b**: 3) were extracted from 2D-DQF-COSY [52] and simple ^{1}H-1D spectra. All molecules were measured in (D_6)DMSO.

Structure Calculations and Molecular Modelling. Distance geometry (DG) and molecular dynamics-simulated annealing (MD-SA) calculations were performed with the INSIGHT II (version 98.0) software package from *MSI* on *Silicon Graphics O2 R5000* computers. A hundred structures were generated from the distance-bound matrices. Triangle-bound smoothing was used. The NOE intensities were converted into interproton distance constraints by using the following classification: very strong (v*s*) 1.7 – 2.3 Å, strong (*s*) 2.2 – 2.8 Å, medium (*m*) 2.6 – 3.4 Å, weak (*w*) 3.0 – 4.0 Å, very weak (v*w*) 3.2 – 4.8 Å, and the distances of pseudo atoms were corrected as described by *Wüthrich* [49]. The ^3J(HN,Hα) coupling constants were converted into constraints for the backbone ϕ dihedral angles by using the *Karplus* relation. Multiple discrete ranges were used for the ϕ torsion-angle restraints when multiple non-overlapping solutions exist for the *Karplus* equation, taking into account exper. error and 5° uncertainty from the *Karplus* parameters. The structures were generated in four dimensions, then reduced to three dimensions with the EMBED algorithm, and optimized with a simulated

annealing step according to the standard protocol of the DG II package of INSIGHT II. All hundred structures were refined with a short MD-SA protocol: after an initial minimization, 5 ps at 300 K were simulated, followed by exponential cooling to *ca.* 0 K during 10 ps. A time step of 1 fs was used with the CVFF force field while simulating the solvent DMSO with a dielectric constant of 46.7. The exper. constraints were applied at every stage of the calculation with 50 kcal · mol^{-1} · Å^{-2} for distance constraints and 50.0 kcal · mol^{-1} · rad^{-2} for coupling constants. For the ten lowest-energy structures, violations of experimental NOE constraints were all below 0.3 Å. For optimization of the ether linkage between the aromatic rings, computer models for *para-meta* and *meta-para* linkages were generated, and low-energy conformations were calculated by the same combined DG/MDSA approach as described above, however, without experimental constraints. Highly defined structures were obtained by this purely computational approach, probably due to stringent steric requirements for the ring closure.

Kinetic Measurements. The CL, TL, and PGPH activities of yeast proteasome were determined under the following conditions: *i*) CL activity was monitored with 0.34 nM yeast proteasome in 20 mM HEPES buffer (pH 7.5) containing 0.5 mM EDTA, 0.025% SDS, and 5% DMSO, and using 7.5 μM Suc-Leu-Leu-Val-Tyr-AMC (*Bachem*, D-Heidelberg) as fluorogenic substrate (380-nm excitation, 460-nm emission); *ii*) TL activity with 5.6 nM yeast proteasome in 50 mM *Tris*/HCl buffer (pH 7.5) containing 0.5 mM EDTA, 100 mM NaCl, 0.01% *Triton X-100*, and 5% DMSO, and 50 μM Z-Ala-Arg-Arg-AMC (*Bachem*, D-Heidelberg) as fluorogenic substrate (380-nm excitation, 460-nm emission); *iii*) PGPH activity with 3.4 nM yeast proteasome in 50 mM *Tris*/HCl buffer (pH 7.5) containing 0.5 mM EDTA, 100 mM NaCl, 0.001% SDS, 5% DMSO, and 1 mM DTT, and 50 μM Z-Leu-Leu-Glu-β-Na (*Bachem*, D-Heidelberg) as fluorogenic substrate (345-nm excitation, 425-nm emission). Based on previous reports [53], the detergents were optimized for each activity. The enzyme assays were carried out at 37° in a total volume of 500 μl on a *SFM 25* spectrofluorimeter (*Biotek-Kontron*, D-Neufahrn). Inhibitors were dissolved in DMSO and used at 1–300 μM concentration in the assay. The K_i values were derived by non-linear regression analysis of the experimental v_i/v_0 data points and inhibitor concentrations, and fitting to the equation for classical inhibition ($v_i/v_0 = 1/(1 + I_t/K_i)$). When inhibition of the proteasome activity was not observed, K_i values were assumed to be at least tenfold higher than the highest inhibitor concentration used, *i.e.*, $\geq$2000 μM. Since the enzyme activities were measured at substrate concentrations $<$ K_m, correction for substrate competition was not required.

This work was supported by the grants A2 and A6 of the SFB 469 of the Ludwig-Maximilians-Universität, Munich.

REFERENCES

[1] J. Adams, *Trends Mol. Med.* **2002**, *8*, S49.
[2] A. F. Kisselev, A. L. Goldberg, *Chem. Biol.* **2001**, *8*, 739.
[3] K. L. Rock, A. L. Goldberg, *Annu. Rev. Immunol.* **1999**, *17*, 739.
[4] J. Myung, K. B. Kim, C. M. Crews, *Med. Res. Rev.* **2001**, *21*, 245.
[5] A. L. Goldberg, K. Rock, *Nat. Med.* **2002**, *8*, 338.
[6] D. Voges, P. Zwickl, W. Baumeister, *Annu. Rev. Biochem*. **1999**, 68, 1015.
[7] M. Bochtler, L. Ditzel, M. Groll, C. Hartmann, R. Huber, *Annu. Rev. Biophys. Biomol. Struct*. **1999**, *28*, 295.
[8] M. Groll, R. Huber, *Int. J. Biochem. Cell Biol.* **2003**, *35*, 606.
[9] J. Löwe, D. Stock, B. Jap, P. Zwickl, W. Baumeister, R. Huber, *Science* **1995**, *268*, 533.
[10] M. Groll, H. Brandstetter, H. Bartunik, G. Bourenkow, R. Huber, *J. Mol. Biol.* **2003**, *327*, 75.
[11] M. Groll, L. Ditzel, J. Löwe, D. Stock, M. Bochtler, H. D. Bartunik, R. Huber, *Nature* **1997**, *386*, 463.
[12] F. Kopp, K. B. Hendil, B. Dahlmann, P. Kristensen, A. Sobek, W. Uerkvitz, *Proc. Natl. Acad. Sci. U.S.A.* **1997**, *94*, 2939.
[13] L. Ditzel, R. Huber, K. Mann, W. Heinemeyer, D. H. Wolf, M. Groll, *J. Biol. Chem.* **1998**, *279*, 1187.
[14] M. Groll, W. Heinemeyer, S. Jäger, T. Ullrich, M. Bochtler, D. H. Wolf, R. Huber, *Proc. Natl. Acad. Sci. U.S.A.* **1999**, *96*, 10976.
[15] W. Heinemeyer, M. Fischer, T. Krimmer, U. Stachon, D. H. Wolf, *J. Biol. Chem.* **1997**, *272*, 25200.
[16] M. Orlowski, S. Wilk, *Arch. Biochem. Biophys.* **2000**, *383*, 1.
[17] K. L. Rock, C. Gramm, L. Rothstein, K. Clark, R. Stein, L. Dick, D. Hwang, A. L. Goldberg, *Cell* **1994**, *78*, 761.

[18] J. Adams, M. Behnke, S. Chen, A. A. Cruickshank, L. R. Dick, L. Grenier, J. M. Klunder, Y.-T. Ma, L. Plamondon, R. L. Stein, *Bioorg. Med. Chem. Lett.* **1998**, *8*, 333.
[19] M. Bogyo, J. S. McMaster, M. Gaczynska, D. Tortorella, A. L. Goldberg, H. Ploegh, *Proc. Natl. Acad. Sci. U.S.A.* **1997**, *94*, 6629.
[20] M. Bogyo, S. Shin, J. S. McMaster, H. Ploegh, *Chem. Biol.* **1998**, *5*, 307.
[21] G. Fenteany, R. F. Standaert, W. S. Lane, S. Choi, E. J. Corey, S. L. Schreiber, *Science* **1995**, 268, 726.
[22] L. Meng, R. Mohan, B. H. B. Kwok, M. Elofsson, N. Sin, C. M. Crews, *Proc. Natl. Acad. Sci. USA* **1999**, *96*, 10403.
[23] L. Meng, B. H. B. Kwok, N. Sin, C. M. Crews, *Cancer Res.* **1999**, *59*, 2798.
[24] Y. Koguchi, J. Kohno, M. Nishio, K. Takahashi, T. Okuda, T. Ohnuki, S. Komatsubara, *J. Antibiot.* **2000**, *53*, 105.
[25] J. Kohno, Y. Koguchi, M. Nishio, K. Nakao, M. Kuroda, R. Shimizu, T. Ohnuki, S. Komatsubara, *J. Org. Chem.* **2000**, *65*, 990.
[26] M. Groll, K. B. Kim, N. Kairies, R. Huber, C. M. Crews, *J. Am. Chem. Soc.* **2000**, *122*, 1237.
[27] M. Groll, Y. Koguchi, R. Huber, J. Kohno, *J. Mol. Biol.* **2001**, *311*, 543.
[28] M. Kaiser, M. Groll, C. Renner, R. Huber, L. Moroder, *Angew. Chem.* **2002**, *114*, 817; *Angew. Chem., Int. Ed.* **2002**, *41*, 780.
[29] M. Kaiser, C. Siciliano, I. Assfalg-Machleidt, M. Groll, A. G. Milbradt, L. Moroder, *Org. Lett.* **2003**, *5*, 3435.
[30] J. W. Janetka, P. Raman, K. Satyshur, G. R. Flentke, D. H. Rich, *J. Am. Chem. Soc.* **1997**, *119*, 441.
[31] J. W. Janetka, K. Satyshur, D. H. Rich, *Acta Crystallogr. Sect. C*, **1996**, *52*, 3112.
[32] G. Müller, H. Giera, *J. Comput.-Aided Mol. Design* **1998**, *12*, 1.
[33] D. L. Boger, Y. Nomoto, B. R. Teegarden, *J. Org. Chem.* **1993**, *58*, 1425.
[34] J. W. Janetka, D. H. Rich, *J. Am. Chem. Soc.* **1997**, *119*, 6488.
[35] A. J. Pearson, G. Bignan, P. Zhang, M. Chelliah, *J. Org. Chem.* **1996**, *61*, 3940.
[36] D. A. Evans, C. J. Dinsmore, A. M. Ratz, D. A. Evrard, J. C. Barrow, *J. Am. Chem. Soc.* **1997**, *119*, 3417.
[37] K. C. Nicolaou, C. N. C. Boddy, S. Natarajan, T.-Y. Yue, H. Li, S. Bräse, J. M. Ramanjulu, *J. Am. Chem. Soc.* **1997**, *119*, 3421.
[38] D. M. T. Chan, K. L. Monaco, R.-P. Wang, M. P. Winters, *Tetrahedron Lett.* **1998**, *39*, 2933.
[39] C. P. Decicco, Y. Song, D. A. Evans, *Org. Lett.* **2001**, *3*, 1029.
[40] R. Beugelmans, A. Bigot, M. Bois-Choussy, J. Zhu, *J. Org. Chem.* **1996**, *61*, 771.
[41] P. J. Krenitsky, D. L. Boger, *Tetrahedron Lett.* **2002**, *43*, 407.
[42] K. Burgess, D. Lim, M. Bois-Choussy, J. Zhu, *Tetrahedron Lett.* **1997**, *38*, 3345.
[43] T. Wenzel, W. Baumeister, *Nature Struct. Biol.* **1995**, *2*, 199.
[44] Z.-Q. Yang, B. H. B. Kwok, S. Lin, M. A. Koldobskiy, C. M. Crews, S. J. Danishefsky, *ChemBioChem*. **2003**, *4*, 508.
[45] H. Kase, M. Kaneko, K. Yamada, *J. Antibiot.* **1987**, *40*, 450.
[46] T. Yasuzawa, K. Shirahata, H. Sano, *J. Antibiot.* **1987**, *40*, 455.
[47] S. Sano, K. Ikai, H. Kuroda, T. Nakamura, A. Obayashi, Y. Ezure, H. Enomoto, *J. Antibiot.* **1986**, *39*, 1674.
[48] S. Sano, H. Kuroda, M. Ueno, Y. Yoshikaewa, T. Nakamura, A. Obayashi, *J. Antibiot.* **1987**, *40*, 519.
[49] K. Wüthrich, 'NMR of Proteins and Nucleic Acids', John Wiley & Sons, New York, 1986.
[50] A. Bax, D. G. Davis, *J. Magn. Reson.* **1985**, *65*, 355.
[51] A. Bax, D. G. Davis, *J. Magn. Reson.* **1985**, *63*, 207.
[52] M. Rance, O. W. Sorensen, G. Bodenhausen, G. Wagner, R. R. Ernst, K. Wüthrich, *Biochem. Biophys. Res. Commun.* **1983**, *117*, 479.
[53] J. Arribas, J. G. Castano, *J. Biol. Chem.* **1990**, *265*, 13969.

Received October 9, 2003